Aquatic Geochemistry (2006) 12: 269–298
DOI 10.1007/s10498-005-6246-7

The Removal of Dissolved Metals by Hydroxysulphate Precipitates during Oxidation and Neutralization of Acid Mine Waters, Iberian Pyrite Belt

J. SÁNCHEZ ESPAÑA[1,★], E. LÓPEZ PAMO[1], E. SANTOFIMIA PASTOR[1], J. REYES ANDRÉS[2] and J.A. MARTÍN RUBÍ[2]
[1]*Dirección de Recursos Minerales y Geoambiente, Instituto Geológico y Minero de España (IGME), Rios Rosas 23, 28003, Madrid, Spain;* [2]*Centro de Laboratorios y Técnicas de Apoyo, Instituto Geológico y Minero de España (IGME), La Calera 1, 28760, Tres Cantos, Spain*

(Received 29 August 2005; accepted 23 December 2005)

Abstract. This study examines the removal of dissolved metals during the oxidation and neutralization of five acid mine drainage (AMD) waters from La Zarza, Lomero, Esperanza, Corta Atalaya and Poderosa mines (Iberian Pyrite Belt, Huelva, Spain). These waters were selected to cover the spectrum of pH (2.2–3.5) and chemical composition (e.g., 319–2,103 mg/L Fe; 2.85–33.3 g/L $SO_4^{=}$) of the IPB mine waters. The experiments were conducted in the laboratory to simulate the geochemical evolution previously recognized in the field. This evolution includes two stages: (1) oxidation of dissolved Fe(II) followed by hydrolysis and precipitation of Fe(III), and (2) progressive pH increase during mixing with fresh waters. Fe(III) precipitates at pH <3.5 (stages 1 and 2) in the form of schwertmannite, whereas Al precipitates during stage 2 at pH 5.0 in the form of several hydroxysulphates of variable composition (hydrobasaluminite, basaluminite, aluminite). During these stages, trace elements are totally or partially sorbed and/or co-precipitated at different rates depending basically on pH, as well as on the activity of the $SO_4^{=}$ anion (which determines the speciation of metals). The general trend for the metals which are chiefly present as aqueous free cations (Pb^{2+}, Zn^{2+}, Cu^{2+}, Cd^{2+}, Mn^{2+}, Co^{2+}, Ni^{2+}) is a progressive sorption at increasing pH. On the other hand, As and V (mainly present as anionic species) are completely scavenged during the oxidation stage at pH <3.5. In waters with high activities ($>10^{-1}$) of the $SO_4^{=}$ ion, some elements like Al, Zn, Cd, Pb and U can also form anionic bisulphate complexes and be significantly sorbed at pH <5. The removal rates at pH 7.0 range from around 100% for As, V, Cu and U, and 60–80% for Pb, to less than 20% for Zn, Co, Ni and Mn. These processes of metal removal represent a significant mechanism of natural attenuation in the IPB.

Key words: acid mine drainage, Fe(III) hydrolysis, schwertmannite, metal sorption, natural attenuation

★ Author for correspondence. E-mail: j.sanchez@igme.es

1. Introduction and Previous Work

The Iberian Pyrite Belt (IPB) province represents an outstanding example of mine water pollution. The volume of acid water generated in the mine sites (estimated in a total of 12 Hm^3 in 2003 only in the Odiel basin; Sánchez-España et al., 2005a), or the extreme composition of some leachates (e.g., pH$\sim$1 and tens of grams per liter of dissolved Fe and $SO_4^{=}$, and grams per liter of Al, Cu, Zn or Mn in waste pile seepage and in the Corta Atalaya pit lake; unpubl.) are good evidences of such drastic contamination.

Recent work carried out in the area (Sánchez-España et al., 2005b, 2006 in press), has shown that the acid-sulphate waters emerging from the mine sites (waste-rock piles, tailings impoundments, mine shafts) evolve geochemically and show a significant self-mitigating capacity of its acidity and metal content. This evolution includes an initial oxidation stage at nearly constant flow rate (first hundreds of meters from the emerging points to the first confluence with a pristine stream course) during which the oxidation of Fe(II) to Fe(III) is catalyzed by iron-oxidizing bacteria. The Fe(III) is subsequently hydrolyzed and precipitated in the form of schwertmannite at pH 2.5–3.5. When the mine waters intersect fresh water courses, a second stage in the AMD evolution occurs in which the pH increase provokes the removal of Fe and, at pH >4.5, the precipitation of Al hydroxysulphates. The formed Fe and Al precipitates have low crystallinity, very small particle size (nano to microcrystalline) and high specific surface area (Bigham et al., 1996; Bigham and Nordstrom, 2000). These physical properties make these minerals very efficient sorbents of metals (Dzombak and Morel, 1990; Stumm and Morgan, 1996; Langmuir, 1997; Smith, 1999). In consequence, their presence as suspended colloids in the water column of streams and lakes affected by AMD can be important in the transport and water-sediment partition of highly toxic trace elements like As, Pb, Cd or Cr. As an example, many schwertmannite particles can be of such low diameter that they can easily pass through conventional 0.45 μm membrane filters (Bigham et al., 1996), so that the metals transported on the mineral surfaces of these particles can be equivocally included in the ''dissolved'' aqueous phase during routinary sampling procedures in the field.

The combination of precipitation, sorption and dilution accounts for the decrease in concentration of dissolved toxic elements, which reduces the environmental impact to the local streams. As an example, Sánchez-España et al. (2005b, in press a, b) have found that up to 70% of the Fe and approaching 95% of the As initially dissolved in the AMD emissions, can be removed from solution at a distance of 1 km or less from the discharge points in some mine sites of the IPB (e.g., La Zarza, Lomero, Esperanza). Among the trace elements, As, Cr, V and Se (which commonly form anionic species under acidic conditions) are readily scavenged at pH <3.5. On the other

hand, the most soluble cations (Cu^{2+}, Cd^{2+}, Co^{2+}, Mn^{2+}, Zn^{2+}) remain essentially as dissolved solutes until the pH is near-neutral.

Several problems related with the sampling procedure (for example, contamination of samples by clay-sized aluminosilicates during sampling of fresh ochreous precipitates from the streambed), field measurements (uncertainty of the estimated flow rates) and analytical techniques (several metals are in concentrations close to or below the detection limits) eventually limit the interpretation of some results (for example, it is still uncertain if the transport of elements like Al, Cd, Cu or Zn at pH < 5 is completely conservative; Sánchez-España et al., 2005b). Moreover, most of the available literature dealing with sorption of metals on hydrous ferric oxides in mine drainage settings have been centered on common divalent metal cations such as Zn^{2+}, Cu^{2+}, Pb^{2+}, Cd^{2+} or Mn^{2+} (see Smith, 1999 and references therein), with little information existing for metals such as Th, U or V. These elements can be present in significant concentrations (i.e., hundreds of μg/L) in the IPB waters (Sánchez-España et al., 2005a).

The scope of this work was to study the natural processes of metal removal which are currently taking place in the AMD systems of the IPB. For this purpose, several oxidation and titration experiments followed by chemical analyses of water samples at different pH target values and chemical/mineralogical analyses of the precipitates, were conducted in the laboratory under constant ambient conditions ($T \sim 25$ °C).

2. Description of the Water Samples

The water samples used for the oxidation and titration experiments (effluents from La Zarza, Lomero, Esperanza, Corta Atalaya and Poderosa mines) were selected to cover the spectrum of known pH (2.2–3.5) and chemical compositions (e.g., 319–2,103 mg/L Fe; 2.85–33.3 g/L $SO_4^{=}$; Table I) of the mine drainage in the IPB (Sánchez-España et al., 2005a). These waters were sampled simultaneously on 8th september 2004. The majority of these mine effluents (except in Corta Atalaya, where the AMD emanates from a waste-rock pile) emerge from mine portals. For the exact location and a detailed field description of these mine effluents the reader is referred to the recent review by Sánchez-España et al. (2005a).

At the moment of sampling, the flow rates of the mine portal effluents were in the order of 0.5–3 L/s, whereas the leachate of the Corta Atalaya waste pile was around 15 L/s. The acidic solutions were mostly anoxic in origin (<1 mg/L dissolved O_2, $<10\%$ sat.) and had low redox conditions (Eh < 600 mV) typical of green, Fe(II)-rich mine waters. The iron dissolved in the acidic mine waters was predominantly ferrous iron ($> 90\%$ Fe(II)). The initial chemical composition of these waters is given in Table I.

Table I. Chemical composition of the five acidic mine waters used for the oxidation and neutralization experiments

AMD sample	pH	SO_4	K	Ca	Mg	Mn	Fe	Al	Cu	Zn	As	Cd	Co	Ni	Pb	Th	Tl	U	V
Units		g/L	mg/L								µg/L								
Lomero	3.25	3.81	11.4	499	418	8.08	319	27.95	0.44	13	b.l.	b.l.	114	0.04	651	b.l.	b.l.	b.l.	b.l.
Esperanza	3.22	2.85	5.095	130.5	155	3.94	709	97.6	15.25	17.05	477	43	652	0.165	35	b.l.	24	11	101
La Zarza	3.46	7.36	4.56	220.5	367	76.6	2,103	184.5	12.45	45.8	2,975	477	1,664	0.79	77.4	b.l.	33	25	231
Poderosa	2.24	7.81	12.75	75.65	123	4.12	2,008	261.5	152	122	4,639	416	1,970	0.13	283	50	47	50	81
Corta Atalaya	3.05	33.3	0.085	186.5	3,397	352	1,888	1,899	173	568	b.l.	2,267	14,068	6.33	234	154	b.l.	437	b.l.

Abbreviations: b.l., below detection limit.

3. Methods

3.1. SAMPLING AND FIELD MEASUREMENTS

A volume of 4 L of unfiltered water was directly taken from every AMD site and stored in polyethylene tanks for the oxidation/titration experiments. In addition, aliquots of these water samples were taken with 60 mL-syringes and 0.45 μm cellulose membrane filters (*Millipore*), stored in 125 ml-polyethylene bottles, acidified to pH <2 with concentrated HNO_3, and refrigerated during transport. These samples were used for the determination of the initial chemical composition of the effluents. The polyethylene bottles were washed with HNO_3 for 12 h prior to sampling. Field parameters such as pH, Eh, temperature (T), dissolved O_2 (DO), and electric conductivity (EC), were measured on site with HANNA portable instruments (probe types HI 9025C, HI 9033 and HI 9025, respectively) properly calibrated against supplied calibration standards (Hanna standard solutions HI 7004 (pH 4.01) and HI 7007 (pH 7.01) for pH; Hanna standard solutions HI 7021 (240 mV) and 7022 (470 mV) for Eh).

The iron speciation was measured on site in 0.45μm-filtered samples. The Fe(II) and Fe(III) concentrations were obtained colorimetrically with HACH titration-based test kits using the digital titration method 8214 of HACH Instruments company (citrate as solution buffer, sodium periodate as Fe(II) oxidant and sulfosalicylic acid as Fe(III) colorimetric detector, with TitraVer® standard solution titration cartridge). The accuracy of this method, calculated by repeated analyses of internal standards, was estimated to be better than $\pm 2\%$ (average of $\pm 1\%$).

3.2. OXIDATION AND TITRATION EXPERIMENTS

With the purpose of reproducing the natural geochemical evolution of the AMD solutions in the laboratory, the experiments were divided in two different stages:

- Oxidation stage: this stage was achieved by opening the tanks in the laboratory, therefore exposing the initially anoxic AMD waters to atmospheric conditions until dissolved Fe(II) had been fully oxidized to Fe(III). The Eh value was daily measured to monitor this process. Once Fe(II) had been oxidized, a water sample was taken from the water surface to evaluate the changes in metal content during this stage. Additionally, samples of ochreous precipitates were collected from either the water surface (film-like precipitate) and/or the bottom of the tanks (sedimented precipitate).
- Neutralization stage: The titrations were carried out after the complete oxidation of Fe(II) in the acidic mine waters (and after removing the solid phases formed during the oxidation stage). An aliquot sample of the La Zarza acidic effluent which was preserved from oxidation (so that dissolved

iron was still chiefly present as Fe(II)) was also neutralized to obtain a characteristic titration curve for this water. This stage was accomplished by dropwise addition of a highly concentrated strong base (NaOH 10 M for gross pH increase and NaOH 1M for fine adjustments and stabilization of pH) with continous pH measurement. The water samples were continously stirred to ensure a good homogenization in the tanks and a complete pH stabilization. The pH was measured with a HANNA laboratory pH meter properly calibrated with pH 4 and 7 buffers supplied by HANNA. To study the sorption of metals by the iron and aluminum compounds, water and precipitate samples were taken at reference pH values of 3.5 (representative of Fe precipitation), 5.0 (Al precipitation) and 7.0 (chemical equilibrium at neutral pH conditions). These target pH values were selected from previous titration studies (see Sánchez-España et al., 2005a, and Figure 2 in this work). The water samples were filtered through 0.45 μm membrane filters. The solids were removed from the tanks (when they were entirely sedimented on the bottom of the tanks and the pH had been stabilized), washed with deionized water and dried at ambient temperature for chemical and XRD analyses.

3.3. ANALYTICAL PROCEDURES

Water samples were analyzed by AAS for Na, K, Mg, Ca, Fe, Cu, Mn, Zn and Al, ICP-AES for Ni, and ICP-MS for As, Cd, Co, Pb, Th, U and V. Sulphate was gravimetrically measured as $BaSO_4$. The accuracy and precision of the analytical methods were verified against certified reference waters (SRM 1643, APG 4073) and close agreement with certified values was achieved for all metals. ^{115}In was used as internal standard for measurements by ICP-MS. The detection limits for trace elements were 100 μg/L for Ni, 10 μg/L for Zn, 2 μg/L for Co and Pb, 1g/L for U, 0.5 μg/L for V, 0.4 μg/L for As, Cd and Cu, and 0.2 μg/L for Th. The detection limits for major cations (Na, K, Ca, Mg, Mn, Fe, Al) was < 1 mg/L in all cases.

Solid samples were analyzed by XRF (PHILIPS 1404) for the elements Si, Al, Fe, Ca, Mn and Mg, elemental analyzer (*Eltra CS-200*) for total S, ICP-MS (after digestion with HNO_3 and H_2O_2) for Cd, Co, Th, U, V and Zn, and AAS for Na, Cu, As and Pb. Certified international reference materials (BCS 175/2, BCS 378, FER-1, FER-2) were used to check the accuracy of the analytical data. The detection limits for trace elements were 10 μg/g for Ni, 2 μg/g for Co, Cu, Th, V and Zn, and 0.2 μg/g for Cd and U.

The solid samples were washed with pure distilled water to avoid the formation of sulphate salts by evaporation of the interstitial waters during drying. The samples were characterized by XRD (PHILIPS PW 1710 diffractometer, Cu*K* radiation (40 kV, 40 mA), SEM (PHILIPS XL-30) and EDS (PV-9900; Universidad Autónoma de Madrid).

3.4. GEOCHEMICAL MODELLING

The PHREEQC code (version 2.7; Parkhurst and Appelo, 1999) was used for calculation of the aqueous speciation of metals in the parent acidic solutions, and for the saturation index (SI) of the AMD waters with respect to selected minerals. The thermodynamic database of PHREEQC was enlarged with data from other geochemical codes (MINTEQA2, WATEQ4F) for speciation of As, V, U and Th, and with data from Bigham et al. (1996) for the solubility of schwertmannite and ferrihydrite.

4. Results and Discussion

The initial aqueous concentrations of major and trace metal ions in the acidic mine waters before the oxidation and titration experiments are given in Table I. The speciation of metal ions in the acidic solutions is reported in Table II, whereas the saturation indices of the mine waters with respect to some selected mineral phases are given in Table III. Finally, the mineral identification and chemical composition of the solid phases formed during the oxidation and titration stages are provided in Table IV.

4.1. GEOCHEMICAL MODELLING

4.1.1. *Aqueous speciation of metals*

The calculated values of ionic strength for the analyzed waters ranged from 0.08 (AMD from Esperanza) to 0.38 (AMD from Corta Atalaya), with an average of 0.19. These ionic strengths are well below the value of 0.7 (typical of seawater) which is conventionally considered as an upper limit for the application of the extended Debye-Hükel and the ion-association equations that PHREEQC incorporates for the calculation of activity coefficients of aqueous solutes (Parkhurst and Appelo, 1999; Alpers and Nordstrom, 1999; Nordstrom, 2004).

The geochemical calculations performed with PHREEQC reveal that, at typical conditions of pH and sulphate concentration in the AMD solutions of the IPB (around pH 2.5–3.5 and 0.1 M $SO_4^{=}$), Fe(III) and Al(III) are chiefly present as sulphate complexes such as $FeSO_4^+$, $Fe(SO_4)_2^-$, $AlSO_4^+$ and $Al(SO_4)_2^-$, with a minor presence of the free aqueous ions Fe^{3+} and Al^{3+}. An example of this characteristic speciation of metals is given in Table II, which reports the calculated speciation of dissolved metal ions in some of the mine waters at pH 3.5 and 25 °C. The metal-sulphate ionic complexes are the dominant dissolved forms under which Fe(III) and Al(III) are present in the solutions at low pH, with the hydroxyl-containing ionic complexes having very minor or negligible presence. As the pH increases, however, the

Table II. Speciation of selected elements in mine waters with distinct molality of the $SO_4^{=}$ anion (LM, Lomero; LZ, La Zarza; CA, Corta Atalaya)

Element	Chemical species	Abundance (in molar %)		
		LM	LZ	CA
	Molality $SO_4^{=} \times 10^{-2}$	4	9.3	36
Al (III)	$AlSO_4^+$	70	63	49
	$Al(SO_4)_2^-$	23	28	47
	Al^{3+}	7	9	4
	$AlHSO_4^{2+}$	<0.1	<0.1	<0.1
	$AlOH^{2+}$	<0.1	<0.1	<0.1
	$Al(OH)_3$	–	–	–
	$Al(OH)_4^-$	–	–	–
Fe (III)	$FeSO_4^+$	44	74	33
	$Fe(SO_4)_2$	18	16	32
	Fe^{3+}	2.5	6	2
	$FeHSO_4^{2+}$	9	2	18
	$FeOH^{2+}$	17	0.2	5
	$Fe_3(OH)_4^{5+}$	1.7	<0.1	7
	$Fe_2(OH)_2^{4+}$	2.6	–	3
	$Fe(OH)_2^+$	9	–	–
Mn (II)	Mn^{2+}	50	58	44
	$MnSO_4$	50	42	56
Cu (II)	Cu^{2+}	52	56	58
	$CuSO_4$	48	44	42
Zn (II)	Zn^{2+}	38	47	22
	$ZnSO_4$	49	38	37
	$Zn(SO_4)_2^{=}$	13	15	40
Cd (II)	Cd^{2+}	–	–	14
	$CdSO_4$	–	–	35
	$Cd(SO_4)_2^{=}$	–	–	51
Pb (II)	Pb^{2+}	23	57	11
	$PbSO_4$	66	27	53
	$Pb(SO_4)_2^{=}$	11	15	36
As (V)	$H_2AsO_4^-$	–	58	–
	H_3AsO_4	–	42	–
V (V)	$H_3V_2O_7^-$	–	28	–
	H_3VO_4	–	14	–
	VO_2^+	–	11	–
	$H_2VO_4^-$	–	10	–
	$VO_2SO_4^-$	–	8	–

Table II. Continued

Element	Chemical species	Abundance (in molar %)		
		LM	LZ	CA
	Molality $SO_4^{=} \times 10^{-2}$	4	9.3	36
U (VI)	UO_2SO_4	43	40	20
	$UO_2(SO_4)_2^{=}$	41	35	75
	UO_2^{2+}	16	25	5

The calculations have been performed with the PHREEQC 2.7 geochemical simulator for conditions of pH = 3.5, pe = 13 and T = 25 °C, and using the concentrations given in Table I as input to the program.

sulphated ions become less abundant and are progressively replaced by the hydroxide forms (e.g., $Fe(OH)_2^+$, $Fe_3(OH)_4^{5+}$), which become dominant at neutral conditions. The divalent metal cations (Mn^{2+}, Cu^{2+}, Zn^{2+}, Pb^{2+}) can be present either as free aqueous ions or as sulphate species. Other elements like arsenic and vanadium should be mainly present as oxidized As(V) species (arsenates) and V(V) species (vanadates) like $H_2AsO_4^-$ (or H_3AsO_4) and $H_3V_2O_7^-$.

The importance of the activity of the $SO_4^{=}$ anion on the speciation of some metals is also illustrated in Table II. At low pH and sulphate activities of around 10^{-4} to 10^{-2} (i.e., around 10 to 1,000 mg/L $SO_4^{=}$), which are typical of many AMD waters, most metals are present as free aqueous ions such as Al^{3+} or Zn^{2+}. However, at higher activities of the $SO_4^{=}$ ion, such as those of the studied waters (the measured sulphate concentrations correspond to activities of around 10^{-2} to higher than 10^{-1}), some elements like Al, Zn, Cd, Pb or U can form bisulphate anionic species ($Al(SO_4)_2^-$, $Zn(SO_4)_2^{=}$, $Cd(SO_4)_2^{=}$, $Pb(SO_4)_2^{=}$, $UO_2(SO_4)_2^{=}$). These species are present at significant proportions in the studied waters (see Table II), and can be even predominant at very high sulphate concentrations (as is the case of the Corta Atalaya effluent, with 33 g/L $SO_4^{=}$). This characteristic speciation has profound implications in the behaviour of these metals during the oxidation and neutralization of the mine waters, as the anionic species tend to be adsorbed by the positively charged mineral surfaces at low pH (Dzombak and Morel, 1990; Smith, 1999). In consequence, elements such as Al, Zn, Cd or U, which are normally conservative under acidic conditions, can be partially sorbed and retained in the solid phase (this is discussed in Section 4.3.3).

4.1.2. *Saturation indices of metal oxides/hydroxides/hydroxysulphates*

At low pH, the acidic solutions are commonly saturated with respect to a number of iron minerals like jarosite, schwertmannite and goethite (Table III),

Table III. Saturation index (SI) values for selected compounds under pH 3.5, 5.0 and 7.0 in the La Zarza mine effluent sample (calculated with PHREEQC 2.7)

Mineral	Formula	pH 3.5	pH 5.0	pH 7.0
Fe minerals				
Schwertmannite	$Fe_8O_8(SO_4)(OH)_6$	33	21	31
Ferrihydrite	$Fe_5HO_8 4H_2O$	−0.15	−0.06	1.67
K-jarosite	$KFe_3(SO_4)_2(OH)_6$	14.8	–	–
Goethite	FeOOH	5.59	4.51	6.24
Al minerals				
Basaluminite	$Al_4SO_4(OH)_{10}$	−6.23	3.17	5.83
Gibbsite	$Al(OH)_3$	−1.69	1.39	3.06
Alunite	$KAl_3(SO_4)_2(OH)_6$	2.07	8.92	7.92
Natroalunite	$NaAl_3(SO_4)_2(OH)_6$	2.15	7.82	9.02
Jurbanite	$AlSO_4OH$	0.76	0.92	−1.41
Metal oxides/hydroxides/sulphates				
Manganite	MnO(OH)	−5.37	−0.92	5.08
Hausmantite	Mn_3O_4	−17	−5.27	10.72
Pyrolusite	MnO_2	−0.5	1.36	9.36
Birnessite	MnO_2	−7.2	−1.2	7.31
Bixbyite	Mn_2O_3	−10.56	−1.57	10.45
Tenorite	CuO	−3.32	−1.53	4.72
Antlerite	$Cu_3(OH)_4SO_4$	−6.47	−1.43	5.93
Brochantite	$Cu_4(OH)_6SO_4$	−8.97	−3.27	8.92
$Zn(OH)_2$	$Zn(OH)_2$	−8	−5.57	−1.57
$Pb(OH)_2$	$Pb(OH)_2$	−7	−3.46	0.53
$Cd(OH)_2$	$Cd(OH)_2$	−15	−10.04	−6.04
Anglesite	$PbSO_4$	0.68	0.7	0.7

Negative SI values reflect undersaturation of the AMD water with respect to a given mineral, whereas positive values are indicative of saturation and tendency for precipitation.

although schwertmannite is normally the mineral favoured to precipitate at pH 3.5 and high redox conditions (Eh >700 mV). The example of Table III illustrates the saturation index (SI) values of the water from La Zarza with respect to some selected metal oxides, hydroxides and hydroxysulphates at different pH values. This water (as well as the rest of AMD samples) is strongly saturated with respect to schwertmannite, which has been recognized in the precipitates obtained at pH <3.5 from all the mine waters.

Regarding the Al minerals, PHREEQC predicts the saturation with respect to alunite and natroalunite in the pH range 3.5–7.0, which is in agreement with the stability fields proposed by Nordstrom (1982) for this mineral. This phase, however, has not been identified during the neutralization of the mine

Table IV. Chemical composition of the precipitates obtained in the 5 acidic mine waters during the oxidation (Fe oxid.) and neutralization stages at different pH values

MDM sample	Mineralogy[a]	SiO_2	Al_2O_3	Fe_2O_3	CaO	MnO	MgO	Na_2O	LOI	S	Total[b]	As	Cd	Co	Cu	Ni	Pb	Th	Tl	U	V	Zn
La Zarza																						
Fe oxid. (film precipitate)	Schw (±Gyp)	0.21	0.13	58.44	0.34	0.04	0.12	0.08	40.61	5.35	99.76	298	b.l.	11.9	55	3.45	b.d.	30.6	0.26	1.2	129	129
Fe oxid. (bottom precipitate)	Schw	b.l.	0.64	57.78	0.41	0.07	0.34	0.05	40.58	5.84	99.87	1,007	2.5	14.5	72	3.67	b.l.	b.l.	0.35	b.l.	133	211
pH 3,5	Schw (±Gyp)	0.19	1.90	54.18	0.30	0.18	0.22	0.67	42.36	5.61	99.82	27.4	0.75	17.1	158	4.44	b.l.	b.l.	0.29	0.21	3.8	218
pH 5	Bas	2.64	38.03	b.l.	0.41	0.48	0.48	1.25	56.69	6.85	99.99	2.61	1.7	35	752	11.1	28.1	b.l.	b.l.	b.l.	4.4	446
pH 7	n.i.	b.l.	18.50	0.07	1.08	0.92	1.78	b.l.	b.l.	b.l.	-	15.4	45	909	91,506	289	135	b.l.	4.4	131	b.l.	42,487
Lomero																						
Fe oxid. (bottom precipitate)	Schw	b.l.	b.l.	58.86	2.38	0.02	0.37	0.15	38.08	5.77	99.86	43.1	b.l.	4.3	13.4	0.39	53	b.l.	b.l.	b.l.	5.7	88.2
pH 3,5	Schw	0.36	1.05	54.48	1.50	0.06	0.28	0.22	39.04	5.86	96.62	4.07	3	5.9	72.7	0.6	376	0.23	0.2	b.l.	b.l.	97.7
pH 5	Hybs	n.a.	n.a.	n.a.	n.a.	n.a.	n.a.	n.a.	n.a.	4.77	-	2.45	b.l.	8.6	538	3.99	385	b.l.	0.5	2.8	b.l.	865
pH 7	Gyp	b.l.	5.28	0.11	23.40	0.32	1.18	b.l.	b.l.	b.l.	-	11.7	4.3	14.2	6,171	34.9	6,177	b.l.	b.l.	4.6	0.78	7,773
Esperanza																						
Fe oxid. (bottom precipitate)	Schw (±Gyp)	b.l.	0.27	59.51	0.39	0.02	0.17	0.07	39.51	5.18	99.94	381	0.7	12.4	138	1.32	b.l.	b.l.	0.27	b.l.	159	117
pH 3,5	Schw	0.30	0.86	57.14	0.24	0.03	0.11	0.30	41.03	5.17	99.70	3.55	b.l.	6.6	388	1.13	8.53	0.75	1.7	b.l.	1.2	725
pH 5	Hybs	3.63	39.98	b.l.	0.34	0.04	0.33	0.55	55.13	5.47	99.99	2.16	0.95	13.6	1,430	4.69	2.43	0.38	0.57	7.1	b.l.	258
pH 7	n.i.	b.l.	8.06	0.09	0.66	0.37	4.71	n.a.	n.a.	n.a.	-	10.8	52.3	1,148	43,755	138	123	b.l.	13.9	76.1	b.l.	36,571
Corta Atalaya																						
Fe oxid. (film precipitate)	Schw (±Gyp)	0.10	1.73	52.57	0.78	0.16	1.48	b.l.	b.l.	7.44	-	8.98	6.0	52.4	596	19.9	b.d.	37.9	b.l.	2.2	39.4	1,718
Fe oxid. (bottom precipitate)	Schw	0.18	3.09	43.49	0.75	0.24	2.25	0.05	49.81	8.63	99.69	14.3	8.4	86.9	904	28.8	b.d.	0.94	b.l.	1.4	33.0	2,787
pH 3,5	Schw (±Gyp±Al ox.)	0.18	10.23	37.43	0.34	0.24	1.30	0.89	49.37	7.55	99.79	2.82	b.l.	27.5	1,133	18.2	16.5	11.3	b.l.	1.3	1.3	1,865
pH 5	Alum	0.74	25.00	b.l.	0.59	0.48	3.45	4.85	54.22	9.88	89.34	3.76	13	192	7,955	86.6	b.d.	3.5	b.l.	16.2	0.54	10,794
pH 7	n.i.	b.l.	3.48	0.07	0.69	1.50	6.43	4.73	40.78	b.l.	-	4.82	59.1	2,154	65,762	909	43.9	0.8	b.l.	96.4	0.31	170,919
Poderosa																						
pH 3,5	Schw	0.20	2.22	54.28	0.25	0.03	0.17	1.12	41.64	5.41	99.71	670	4.4	28.2	1,965	3.27	b.l.	6.7	0.54	0.32	23.9	687
pH 5	Bas	1.44	33.03	b.l.	0.27	0.03	0.55	2.17	57.01	6.22	94.50	4.44	3.3	60.7	10,874	5.4	1.23	1.9	0.23	6.4	0.33	2,288
pH 7	n.i.	b.l.	6.83	0.02	0.37	0.08	0.94	2.40	36.30	b.l.	-	8.68	61.3	262	297,981	25.3	16.5	b.l.	1.8	69.1	b.l.	23,285

Major oxides in wt.% and trace elements in ppm. [a]Major mineral phases deduced from XRD; [b]Total oxides excluding sulphur. *Abbreviations:* Schw, schwertmannite; Hybs, hydrobasaluminite; Bas, basaluminite; Alum, aluminite; Gyp, gypsum; Al ox., Al hydrous oxides; LOI, Loss on Ignition at 950 ºC (includes H_2O and SO_3); b.l., below detection limit; n.a., not analyzed; n.i., not identified.

waters. Some jurbanite could theoretically form under pH < 5, as deduced by its slightly positive SI values, although the formation of this mineral under such acidic conditions has been recently questioned by Bigham and Nordstrom (2000). The precipitation of Al above pH 5.0 would mainly take place in the form of basaluminite (or its precursor hydrobasaluminite; see below), although some precipitation of gibbsite could also take place at pH >5.

Finally, the calculations indicate that the coprecipitation (along with schwertmannite or basaluminite) of metals like Cu, Zn, Pb, Cd or Mn as oxides or hydroxides is highly unlikely below pH 5.0, as deduced by their very negative SI values. At pH 7.0, however, PHREEQC predicts oversaturation and possible precipitation of Mn (as manganite, pyrolusite or hausmantite) and Cu (as tenorite or antlerite) (Table III). Some carbonate phases which were also included in the calculations (such as rhodochrosite, cerussite, otavite, siderite or smithsonite; data not shown) displayed always negative SI even at pH 7.

4.2. METAL REMOVAL DURING THE OXIDATION STAGE

The oxidation of Fe(II) to Fe(III) was completed in all the mine waters after a time span of between 1 and 2 weeks. A thick layer of iron-rich ochreous precipitate was deposited on the bottom of the tanks in all AMD solutions except in the Poderosa mine effluent (which had a pH of 2.2). The XRD studies have determined that these precipitates are basically composed of schwertmannite ($Fe_8O_8(SO_4)(OH)_6$; Bigham et al., 1996; Table IV), occasionally with some trace gypsum. In the samples from Corta Atalaya and La Zarza, a second type of schwertmannite precipitate was formed as a very thin film on the water surface.

The oxidation of Fe(II) through reaction 1 consumes one hydrogen ion per mol of Fe(II) oxidized, whereas the formation of schwertmannite through reaction 2 (Bigham et al., 1996) releases 2.75 mol of hydrogen ions per mol of Fe(III) hydrolized:

$$Fe^{2+} + 1/4O_2\ (g)\ + H^+ \Leftrightarrow Fe^{3+} + 1/2H_2O, \tag{1}$$

$$8Fe^{3+} + SO_4^{=} + 14H_2O \Leftrightarrow Fe_8O_8(SO_4)(OH)_6 + 22H^+. \tag{2}$$

Therefore, the overall balance between oxidation of Fe(II) and hydrolysis of Fe(III) provokes a strong acidification of the aqueous solutions (all the mine waters with pH >3 experienced a pH decrease to around 2.3 during this stage). These observations are in agreement with the predictions of Nordstrom (2004) and had been already recognized in many AMD streams of the area (Sánchez-España et al., in press a,b).

The progressive decrease in the aqueous metal concentrations through processes of adsorption and/or coprecipitation (hereafter referred to collectively as sorption) is illustrated in Figure 1. Considering the pre- and post-oxidation composition of the mine water samples, it is concluded that the precipitation of schwertmannite accounts for a very significant scavenging of Fe(III) and other elements like As and V. On the other hand, other metals like Al, Cu and Zn behave conservatively during this stage.

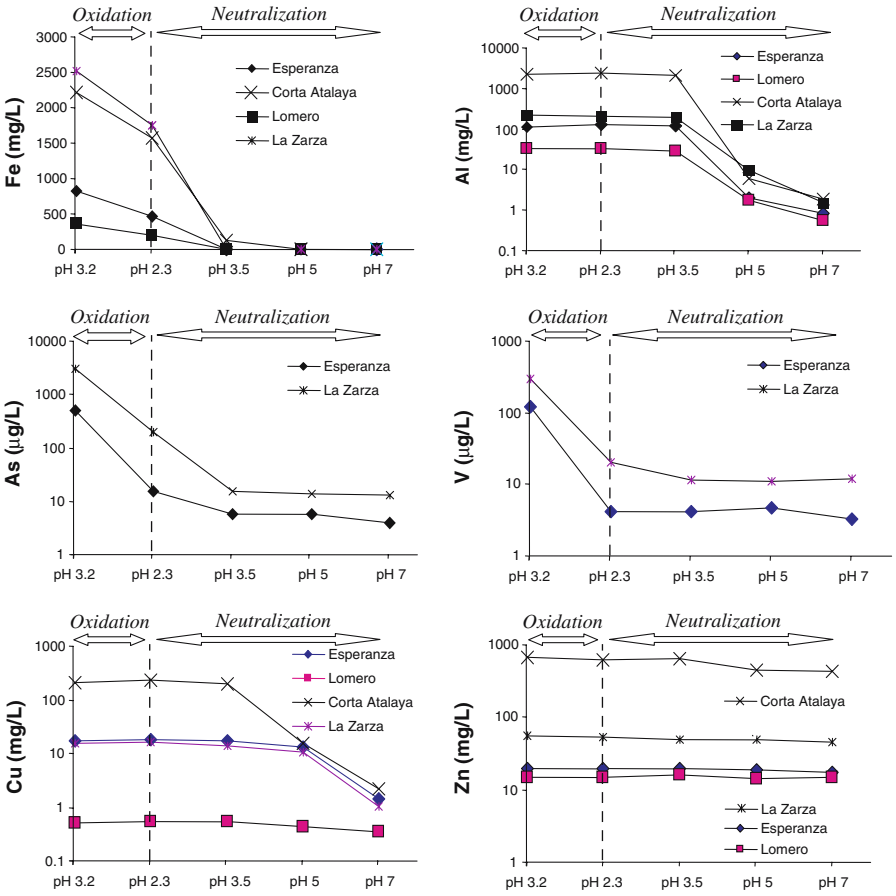

Figure 1. Variation in the concentration of dissolved metals and arsenic in the acid mine waters during the oxidation and neutralization stages (these two processes are separated by dashed lines). Note that Fe and Al are decreased by precipitation of schwertmannite (pH 3.5) and Al hydroxysulphates (pH 5.0), respectively, whereas As and V are removed from the aqueous phase by sorption (mainly during oxidation) onto the formed Fe colloids. In contrast, with the exception of the mine water from Corta Atalaya, Cu remains in solution until pH 7.0 (when it is significantly scavenged), and Zn behaves essentially as conservative along the entire neutralization process.

Iron is significantly removed from solution in all the mine waters (precipitation of 43% of the initial Fe content in Esperanza, 47% in Lomero, and around 30% in Corta Atalaya and La Zarza mine effluents). Similarly, As and V were almost completely scavenged from the aqueous phase by sorptive processses during the oxidation stage (removal of 93–97% of As and V in the waters from Esperanza and La Zarza). This finding is in agreement with the high As and V concentrations found in the schwertmannite precipitates of the oxidation stage in comparison with those of the schwertmannites formed by neutralization (Table IV), and seems coherent with the speciation of these elements (predominantly present as anionic species) in the aqueous solutions.

The rapid scavenging of As near its source by sorption on hydrous iron oxides has been widely documented (e.g., Chapman et al., 1983; Filipek et al., 1987; Leblanc et al., 1996; Carlson et al., 2002; Fukushi et al., 2003; Casiot et al., 2003). Because of its toxicity (As is a known carcinogenic element) and its abundance in the massive mineralizations of the IPB (As is a major constituent in arsenopyrite and cobaltite, and a trace element in pyrite), the rapid As retention is of great environmental concern. Fukushi et al. (2003) state that the As(V) uptake by schwertmannite takes place by either coprecipitation (displacing structural SO_4 in the schwertmannite stoichiometry) and post-precipitation sorption (via ligand exchange with SO_4), whereas Regenspurg and Peiffer (2005) have reported important substitutions of sulphate by arsenate in schwertmannite. Therefore, As could have been either coprecipitated and/or sorbed by schwertmannite during oxidation.

In comparison with the bottom precipitates, the film-like schwertmannite found in the waters from La Zarza and Corta Atalaya shows a higher $(Fe/S)_{molar}$ ratio and lower metal content. An exception to this trend is the case of Th and U (Table IV). These elements were present in the AMD sample from Corta Atalaya at concentrations of 437 and 154 μg/L, respectively (Table I), although they can be present at higher concentrations (up to 1,100 μg/L U and 400 μg/L Th; Sánchez-España et al., 2005a). Thorium can be present as Th(IV) species such as $Th(SO_4)_2$ under acid-sulphate conditions (Langmuir, 1997), whereas uranium can be present as U(VI) species such as UO_2SO_4 or $(UO_2SO_4)_2^=$ in oxidized mine waters (Table II). Among these two elements, Th seems to have been specially retained in the film-like precipitate.

4.3. METAL REMOVAL DURING THE NEUTRALIZATION STAGE

4.3.1. *Preliminar titration studies: the Fe and Al buffers*

The titration of a strong acid by addition of a strong base (such as NaOH) is a useful tool for the identification of buffer reactions in aqueous systems (Stumm and Morgan, 1996; Langmuir, 1997). Several recent examples of the

successful application of this tool on the modelling of mine waters can be found in Fyson and Kalin (2000) or Totsche et al. (2003).

Based on previous titration studies (Sánchez-España et al., 2005a), the Fe and Al buffer systems have been well recognized in the AMD systems of the IPB (Figure 2). The titration curve of a typical acid mine water with significant amounts of dissolved Fe(III) and Al shows two inflection points (followed by their respective *plateaus*) at pH $\sim$3.0 and $\sim$4.5 (Figure 2a). The mineral acidity released during the hydrolysis of Fe(III) and Al, respectively,

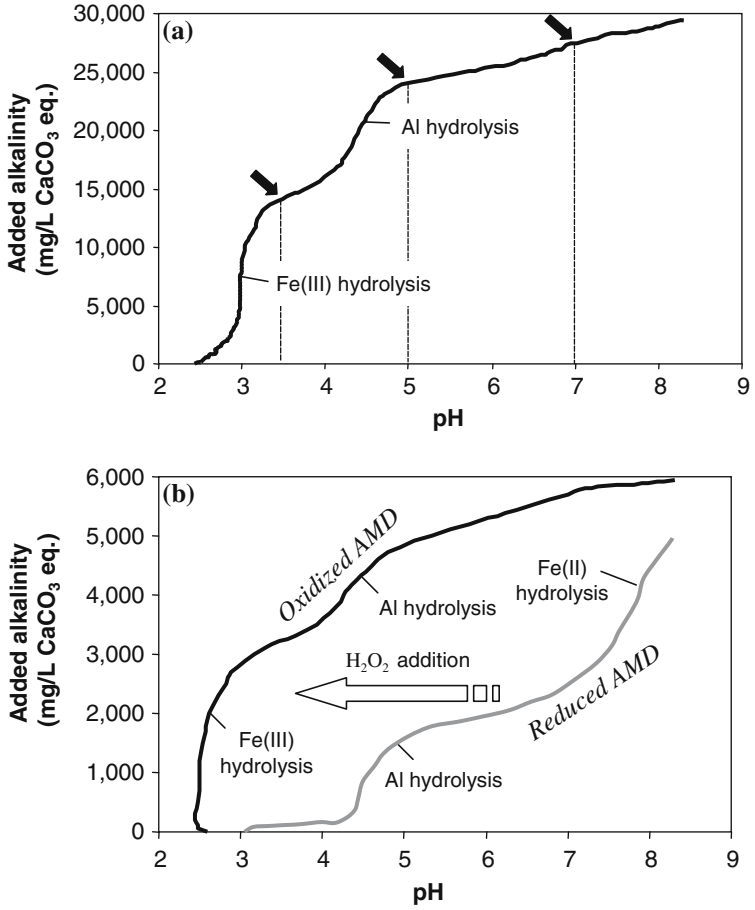

Figure 2. Examples of titration curves for the IPB acid mine waters: (a) titration curve of the Corta Atalaya mine effluent, showing the typical sigmoid shape of an oxidized mine water (100% Fe(III), 0% Fe(II)) with the two inflection points corresponding with the hydrolysis of Fe(III) and Al (the dashed lines and black arrows indicate the pH values at which the water and precipitate samples were taken during titration). (b) Titration curves for the La Zarza AMD sample, showing the effect of the addition of H_2O_2 to a reduced water (100% Fe(II)) to completely oxidize Fe(II).

provokes a strong buffering in the waters. The existing *plateaus* at pH >3.5 and pH >5 suggest that Fe and Al have been almost totally hydrolyzed and precipitated at these pH values. The *ferric* (Fe(III)-rich, pH <3.5) and *aluminous* (Al(III)-rich, pH <5) hydrogeochemical facies have been well recognized in many AMD settings of the IPB (Sánchez-España et al., 2005a, b) and lead to the spatial and temporal separation of precipitating phases of hydrolyzed iron and aluminum in the mine waters of the area. If not previously oxidized, Fe(II) will be hydrolyzed (thus provoking additional buffering) at around pH 7.5–8.0 (Figure 2b).

4.3.2. *Mineral characterization of the precipitates formed at pH 3.5, 5 and 7*

The mineral and chemical composition of the precipitates obtained during the titration process are provided in Table IV and Figure 3. Schwertmannite is ubiquitous as the primary precipitating mineral during the hydrolysis of Fe(III) at pH <3.5. This oxyhydroxysulphate shows typical XRD patterns with 8 bands at 1.46, 1.51, 1.66, 1.95, 2.28, 2.55, 3.39 and 4.86 Å, and average composition of 55–60% Fe_2O_3 and 5.2–5.9% S (with resulting $(Fe/S)_{molar}$ ratio of around 4.0–4.6), which are characteristic of this mineral (Bigham et al., 1996; Bigham and Nordstrom, 2000). In the precipitates obtained from the mine waters with high Ca content (e.g., Lomero, La Zarza, Corta Atalaya; Table I) some gypsum is also present in the precipitate.

The nature of the Al precipitates formed at pH 5.0 is less clear. Excluding the precipitate from the Corta Atalaya effluent (see below), these solids present an average content of around 33–40% Al_2O_3 and 4.8–6.8% S, resulting in $(Al/S)_{molar}$ ratios of 3.5–4.6. These mineral phases are nearly amorphous to XRD, although it is possible to recognize two broad reflections at around 7 and 20 °2θ in the XRD profiles (Figure 3). This diffraction pattern, along with the chemical data, suggests that the Al precipitates probably consist in poorly ordered hydroxysulphates with composition intermediate between basaluminite ($Al_4(SO_4)(OH)_{10}{\cdot}5H_2O$) and hydrobasaluminite ($Al_4(SO_4)(OH)_{10}{\cdot}12$–$36H_2O$). The chemical data of the Al precipitate obtained in the Esperanza and Lomero AMD could correspond to a partly dehydrated hydrobasaluminite (ideally, 5% S, 32% Al_2O_3 and $(Al/S)_{molar}=4$; Bannister and Hollingworth, 1948; Basset and Goodwin, 1949; Bigham and Nordstrom, 2000), whereas those obtained from the waters of La Zarza and Poderosa are closer to the ideal formula of basaluminite (6.9% S, 44% Al_2O_3, $(Al/S)_{molar}=4$), although probably contaminated with adsorbed silica. The high sodium contents of these solids (0.5–2.2% Na_2O) and the calculations of saturation indices (Table III) suggest that some natroalunite ($NaAl_3(SO_4)_2(OH)_6$) could have also precipitated, although this mineral has not been identified by XRD. The most probable explanation is that the Al precipitates comprise a mixture of several hydroxysulphates with

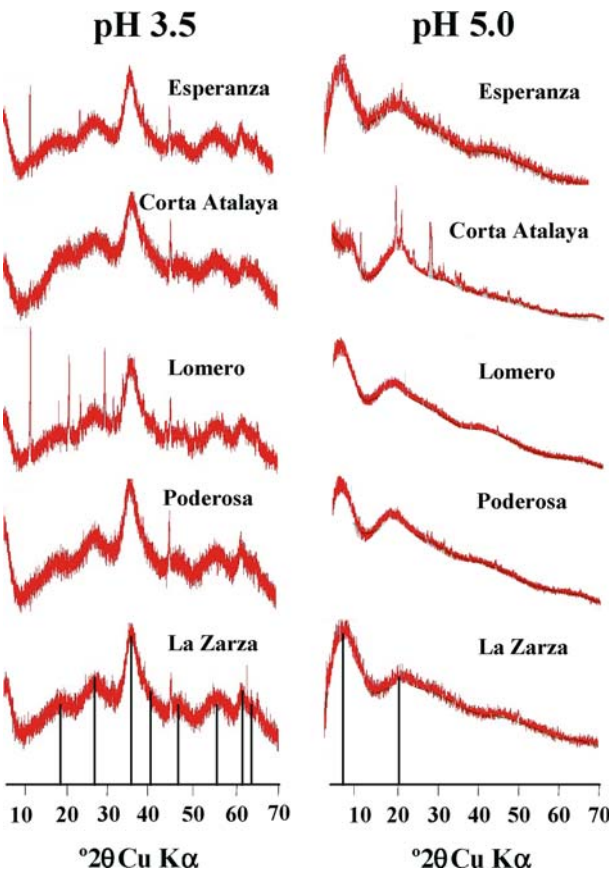

Figure 3. XRD patterns of the precipitates obtained at pH 3.5 and 5.0 during titration of the five mine water samples. Solid lines indicate the main reflections.

distinct stoichiometry, intermediate between hydrobasaluminite and basaluminite.

These observations are in agreement with the geochemical calculations discussed above (Table III), which predict saturation of the acidic solutions with respect to several Al phases (including basaluminite, but also alunite, natroalunite, jurbanite and gibbsite) at pH 5. Also, the results agree with the findings of Adams and Rawajfih (1977), who identified basaluminite and alunite precipitating in acid soils, as well as with published work by Chapman et al. (1983), Berger et al. (2000), and Kim and Kim (2003), who interpreted as amorphous to poorly crystalline basaluminite and/or hydrobasaluminite the natural Al precipitates formed in AMD from Australia, New Mexico, and Korea, respectively, and with data from Totsche et al. (2003), who studied the Al precipitates formed by neutralization of acidic waters from pit lakes in Lusatia, Germany, and obtained a mixture of several Al

hydroxysulphates with variable stoichiometry. In addition, Nordstrom and Alpers (1999) and Bigham and Nordstrom (2000), also conclude that a poorly ordered hydrobasaluminite is the most probable mineral phase under which Al precipitates from acid sulphate solutions at pH around 5.0.

The mineral hydrobasaluminite is a metastable precursor of the more stable phase basaluminite ($Al_4(SO_4)(OH)_{10}{\cdot}5H_2O$), which forms by dehydration of the former (Bannister and Hollingworth, 1948; Clayton, 1980; Nordstrom, 1982). Basaluminite is a common Al hydroxysulphate found in mine drainage environments (Nordstrom et al., 1984; Bigham and Nordstrom, 2000), although it is also metastable and tends to be transformed to alunite during maturation or heating (Adams and Rawajfih, 1977; Nordstrom, 1982). The hydrolysis reaction of Al^{3+} to form hydrobasaluminite can be written as follows:

$$4Al^{3+} + SO_4^{=} + 22 - 46\ H_2O \Leftrightarrow Al_4(SO_4)(OH)_{10} \cdot 12 - 36H_2O + 10H^+ \quad (3)$$

Finally, the precipitates obtained at pH 7.0 have not been unequivocally identified by XRD, although both the calculated saturation indices (Table III) and the chemical analyses (Table IV) suggest that they must be a mixture of Al precipitates (residual Al not precipitated during the previous titration step, probably in the form of either basaluminite-hydrobasaluminite or gibbsite, $Al(OH)_3$), together with gypsum (this mineral is predominant in Lomero), and variable contents of oxides-hydroxides-hydroxysulphates of metals such as Mn (likely candidates would be pyrolusite (MnO_2), birnessite (MnO_2), bixbyite (Mn_2O_3), hausmanite (Mn_3O_4), or manganite (MnOOH)) and Cu (probably as tenorite (CuO), antlerite ($Cu_3(OH)_4SO_4$) or brochantite ($Cu_4(OH)_6SO_4$)). The formation of gypsum (pK = 5.9) is coherent, as this mineral commonly precipitates from Ca and sulphate-rich waters at near-neutral conditions. Additionally, the high Mg concentrations found in the pH 7 precipitates (in the range 0.9–6.4%) can be explained in terms of co-precipitation (as $MgAl(OH)_n$) and/or sorption onto the Al precipitates. This possibility has been already described by several authors (Kinniburgh et al., 1976; Baltpurvins et al., 1997; Totsche et al., 2003).

4.3.2.1. *The Corta Atalaya precipitates*. An exception to the above cited mineralogical features is found in the precipitates from the Corta Atalaya effluent. This water shows abnormally high concentrations of Al, Mg and SO_4 compared to the rest of mine waters (Table I), and consequently, the molar ratios of iron to aluminum (Fe:Al $\sim$ 0.5), magnesium (Fe:Mg$\sim$0.25) and sulphur (Fe:S$\sim$0.1) in the parent acid solution are much lower. The resulting precipitate at pH 3.5 contains 10.2% Al_2O_3, 1.3% MgO and 7.55% S, with a $(Fe/S)_{molar}$

ratio of 2.0 which is much lower than that of schwertmannite (~4–5; Bigham et al., 1996). The pH 5 precipitate has an Al_2O_3 content of 25% and $(Al/S)_{molar}$ of 1.6 (that is, very different from that of basaluminite-hydrobasaluminite (~4)).

Schwertmannite is a major constituent in the precipitate of this AMD at pH 2.3–3.5 (as indicated by XRD). However, a more crystalline Fe sulphate also precipitated from this water, although in a lesser extent. This mineral could not be identified by XRD, but it has been detected by SEM and EDS (Figure 4). The precipitation of a white Al colloidal phase (concurrently to the formation of schwertmannite) was also observed during neutralization of this water to pH 3.5. In fact, nearly 15% of the Al initially dissolved in this water was removed from solution during titration to pH 3.5, which suggests either the sorption of Al by schwertmannite and/or the precipitation of an Al-containing phase. The sorption of Al by schwertmannite is discussed later. Regarding the precipitation of Al, this is evidenced in Figure 4 (which shows the presence of small grains of a white and Al-bearing compound surrounding the ferric solid). Thus, it is concluded that the pH < 3.5 precipitates consist in a mixture of schwertmannite with some other Fe and Al hydroxysulphates co-precipitated during titration.

As regards to the Al precipitate obtained at pH 5 (Figure 5), its chemical composition includes 9.88% S and 4.8% Na_2O. These chemical features, along with the XRD profile, suggest that this precipitate is probably formed by aluminite ($Al_2(SO_4)(OH)_4 \cdot 7H_2O$; ideally with 29.6% Al_2O_3 and 9.33% S), with some trace natroalunite and gypsum.

4.3.3. *Sorption of metals during titration*

The sorption edges of selected metals are depicted in Figure 6, and the metal content of the precipitates formed during oxidation and neutralization is illustrated in Figure 7.

4.3.3.1. *Sorption of metal cations.* As previously stated in numerous metal sorption studies (e.g., Kinniburgh and Jackson, 1981; Dzombak and Morel, 1990; Davis and Kent, 1990; Smith et al., 1992; Webster et al., 1998; Smith, 1999; Lee et al., 2002), the sorption edges for all metals display a typical sigmoid shape with increasing sorption at increasing pH, with most of the sorption taking place in the pH range 5–7 (Figure 6).

In addition to pH, the degree of sorption also depends, among other factors, on the amount and type of sorbent formed in the solutions (Dzombak and Morel, 1990; Smith, 1999). From the graphs of Figure 6, it can be stated that the general sorption selectivity sequence for the studied AMD solutions on schwertmannite at pH 3.5 is $As > V > Pb > Cu > U > Co \approx Zn > Mn$. The sorption sequence for the Al hydroxysulphates at pH 5.0 is very similar ($As \approx V > Pb > Cu \approx U > Co \approx Zn > Ni \approx Mn$). In

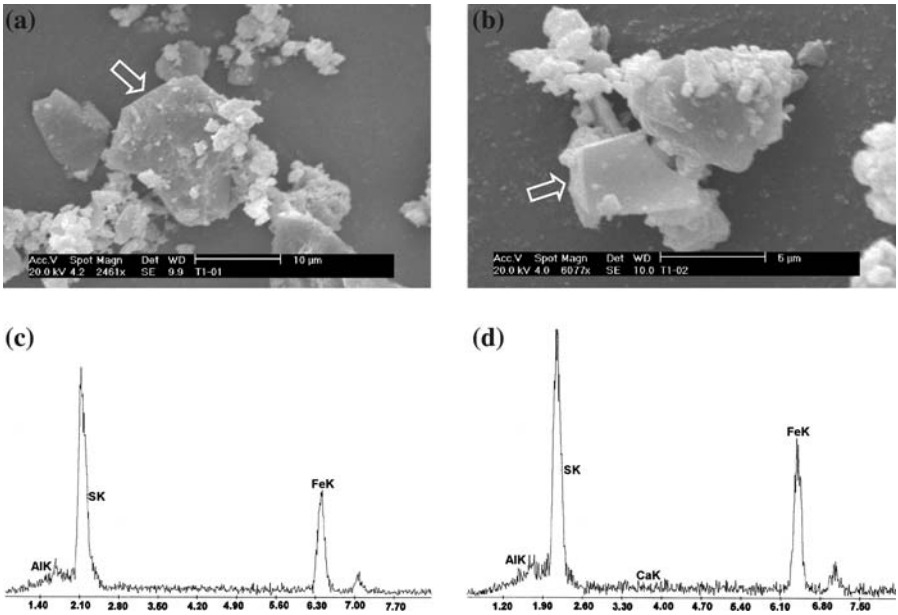

Figure 4. SEM images and EDS patterns of the hydroxysulphate precipitates formed during titration of the Corta Atalaya AMD at pH 3.5. The EDS profiles correspond to the large crystals in the center of the photographs (white arrows). The small, white crystals sorrounding the Fe and S-containing precipitate are a mixture of gypsum and Al compounds. The *X*-axis in the EDS profiles is in KeV.

the only case in which some detectable As and V still remained in solution after the oxidation stage (sample from La Zarza), it is evident that these elements are readily sorbed at pH 3.5 by schwertmannite (removals of 90% for As and 50% for V) and by the Al hydroxysulphates at pH 5.0 (nearly 100% for both elements). Pb shows also a strong affinity to be sorbed by schwertmannite, which can retain between 30% and 70% of dissolved Pb at pH 3.5. Cu is the next metal in the sorption sequence, being significantly adsorbed (around 30–40%) by the Al phases at pH 5.0. At higher pH, some precipitation of Cu oxides/hydroxides/hydroxysulphates could have taken place, as deduced from the saturation indices of Cu minerals at pH 7.0 (Table III) and the concentrations of this element in the precipitates (4–30% wt.; Table IV, Figure 7). An approach from Figure 6 allows to estimate that the pH for 50% sorption (pH_{50}) ranges from 3.1 to 6.5 for Pb, 4.0 to 6.4 for Cu, and 4.2 to 5.8 for U. Thus, nearly 100% of the initially dissolved Cu and U, and up to around 80% of the initial Pb content, had been sorbed and removed from solution at pH 7.

On the other hand, the more soluble metals like Zn, Cd, Mn, Co and Ni remain essentially in solution (sorption of less than 10–15%) at pH 5.0

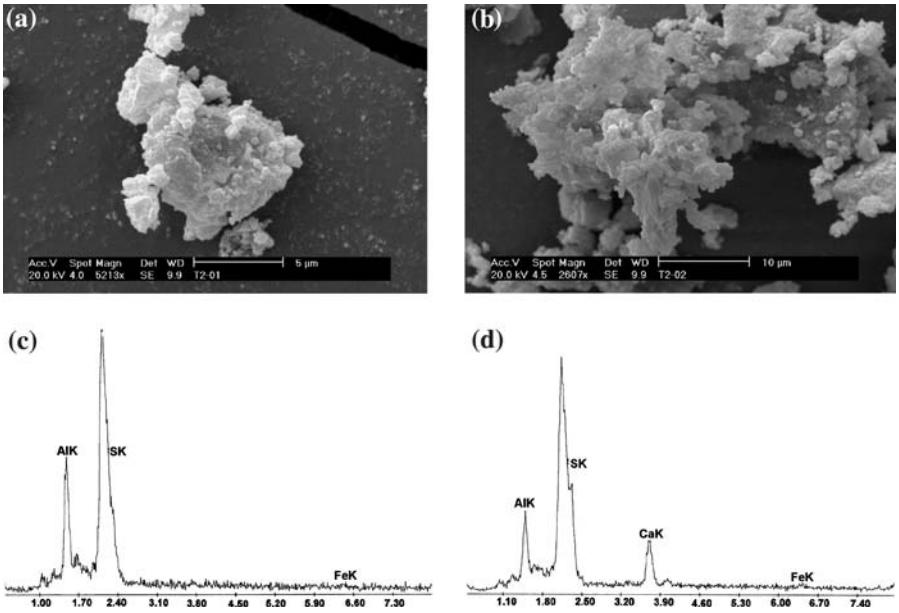

Figure 5. SEM images and EDS patterns of the Al hydroxysulphate precipitate (mixed with gypsum in b-d) obtained during titration of the Corta Atalaya AMD at pH 5.0. The *X*-axis in the EDS profiles is in keV.

(Figure 6). Notwithstanding, a much stronger retention is observed for Zn and Cd (sorption of around 35–40%) at pH 5.0 in the water from Corta Atalaya (this is discussed in the next section). At pH 7.0, a limited sorption of about 10–20% occur for these metals in most of the mine waters, mainly on the formed Al phases, but also on the minor Cu and Mn compounds that could have precipitated at this pH. The high Zn concentrations measured in these precipitates (up to 17% wt.; Table IV) evidence the sorption of this element.

The obtained results also indicate that the degree of sorption depends largely on the amount of sorbent formed during the neutralization process (which depends on the initial chemical composition of the acidic mine waters). For example, the sorption of metals such as Cu, U and Zn at pH 5.0 in the water from La Zarza (0.7 g/L of hydrobasaluminite/basaluminite formed at this pH) is much lower than the sorption of these elements in the sample from Corta Atalaya (8.6 g/L of an aluminite-like precipitate formed at pH 5.0). Further, these two waters show a much stronger sorption for all metals than that observed in the Lomero AMD solution (0.3 g/L of schwertmannite formed at pH < 3.5 and 0.1 g/L of hydrobasaluminite formed at pH 5.0). These data indicate that the composition of the mine effluents strongly determines the grade at which aqueous metal concentrations are naturally attenuated.

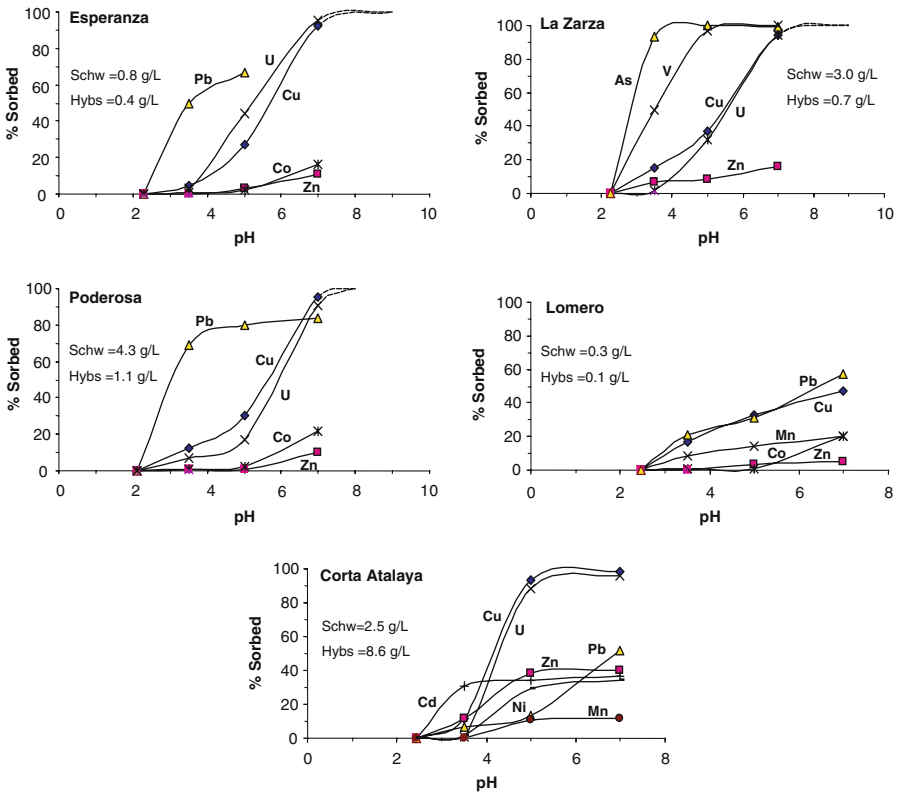

Figure 6. Sorption edges of trace metals and arsenic to the precipitates formed by neutralization of the 5 AMD solutions. The degree of sorption of a given element at a given pH has been calculated by the equation $S_E(\%) = [(C_{Eo}\text{-}C_{Ef})/C_{Eo}] \times 100$, where S_E is the sorption degree of an element E, C_{Eo} is the initial concentration of that element and C_{Ef} is the concentration of the element E at a given pH value. The amount of formed Fe and Al precipitate (given in g/L) has been calculated by assuming that 100% of the initial Fe concentration has precipitated in the form of schwertmannite (Schw) and that 100% of the Al has precipitated as poorly ordered hydrobasaluminite (Hybs). Dashed lines denote extrapolation of the obtained sorption curves to 100% sorption for a given element.

Another observation is the sorption of uranium, which displays a sorption edge very similar to that of Cu in most of the mine waters. The calculated saturation indices for common U minerals (e.g., uraninite, schoepite, tyuyamunite) show always very negative values in the pH range of 3.5–7.0, so that the AMD solutions were always undersaturated with respect to these compounds. Therefore, the coprecipitation of U along with schwertmannite and/or Al minerals is improbable. The uranium mobility in AMD systems is commonly referred to be related with sorptive processes onto Fe and Al oxyhydroxide compounds (Wanty et al., 1999). The similarity between the sorption edges of Cu and U may reflect that the retention of U in the solid

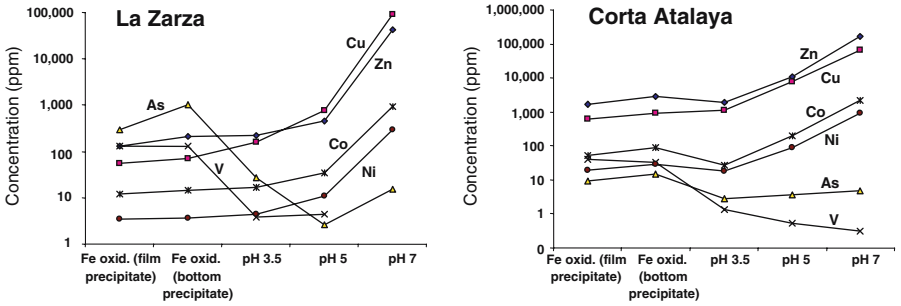

Figure 7. Trace metal and arsenic content (in ppm) of the precipitates formed during oxidation and neutralization of the La Zarza and Corta Atalaya AMD solutions.

phase has taken place via adsorption onto the Al hydroxysulphates in the pH range 5.0–7.0, as well as onto the Cu oxides/hydroxides/hydroxysulphates hypothetically formed at near-neutral conditions. Sorption of this element onto schwertmannite at pH < 3.5 is minimal in comparison with the retention taking place in the Al oxyhydroxysulphates, so that the role of the poorly crystalline Al minerals in the attenuation of U seems to be very important. Although this possibility had been already suggested (e.g., Wanty et al., 1999), the authors are unaware of any prior experimental study which demonstrates the adsorption of U onto Al-oxyhydroxysulphates in mine drainage settings.

Finally, the evolution of the trace element content of the precipitates formed during the oxidation and neutralization stages (Figure 7) is in perfect agreement with the discussed chemical evolution of the aqueous phase. The elements present as anions in the solution (As and V) decrease in concentration as pH increases, whereas Cu, Zn, Co and Ni progressively increased as the pH increased. Thus, a composition trend downstream from the source areas is expected as regards to the metal content of the precipitates deposited on the streambed of the AMDs. The iron precipitates formed in the vicinity of the mining areas at low pH will show high concentrations of As, V and Pb. The schwertmannite-rich films formed on the water surface seem to be enriched in thorium. The aluminum precipitates formed at pH$\sim$5 in the confluence with fresh water courses will show high concentrations in Cu and Zn, and finally, the precipitates formed at near-neutral conditions will show the highest metal concentrations, including Cu, Zn, Co, Ni, Mn and Cd, in addition to other toxic metals like U (Table IV). This downstream evolution of the precipitate composition has been recognized during field studies in the AMD emissions of Tharsis and La Zarza (Sánchez-España et al., 2005b).

4.3.3.2. *Sorption of metal-bisulphate complexes*. As discussed above, some metals like Zn and Cd appear to have been significantly sorbed under low pH, specially in the water from Corta Atalaya (Figure 6). In fact, taking into account the results from the oxidation and neutralization experiments, it seems that not only Zn and Cd, but also Al, could have been significantly sorbed at pH < 5. Aluminum is commonly considered to be conservative at pH < 5 (Nordstrom and Ball, 1986; Nordstrom and Alpers, 1999; Bigham and Nordstrom, 2000), although the results obtained in this study suggest that it has behaved non-conservatively at such acidic conditions. Strong evidences for this statement include: (i) the noticeable decrease in the aqueous Al content during titration to pH 3.5 in all the mine waters (not detectable in Figure 1, but calculated from the chemical analyses: Al removals of 5% in the mine water from Lomero, 8% in Esperanza, and around 15% in the samples from La Zarza, Poderosa and Corta Atalaya), and (ii) the Al_2O_3 concentrations (0.9–3.1 wt.%) detected in the schwertmannite precipitates obtained at pH 3.5. This statement is in agreement with field studies which have reported Al_2O_3 contents in the range of 0.7–1.3 %wt. in many natural schwertmannites precipitated from the IPB mine drainage settings (Sánchez-España et al., 2005a). The SiO_2 content of these samples was very low, so that very little (if any) contamination of aluminosilicates was considered for these samples.

A possible explanation for this apparent non-conservative behaviour of Al, Zn and Cd could be related with the aqueous speciation of these metals in the studied AMD solutions. It has been shown from the PHREEQC calculations on metal speciation (Table II) that Al, Zn and Cd (in addition to Pb and U) can form metal-bisulphate anionic species ($Al(SO_4)_2^-$, $Zn(SO_4)_2^=$, $Cd(SO_4)_2^=$, $Pb(SO_4)_2^=$, $UO_2(SO_4)_2^=$) at the high activities of the $SO_4^=$ ion which commonly present the acid mine waters of the IPB. In fact, these anionic chemical species can be even predominant in the case of the water from Corta Atalaya (Table II) which shows, by far, the highest $SO_4^=$ concentration. These ion complexes could thus be readily sorbed onto the mineral surfaces of the schwertmannite colloids, which commonly show excess of positive charges at low pH (Kinniburgh and Jackson, 1981; Dzombak and Morel, 1990; Smith, 1999).

The effect of the $SO_4^=$ activity on the speciation of metals is illustrated for the case of Al in Figure 8. Under common sulphate activities (10^{-2} to 10^{-4}, as reported in many sorption studies in AMD environments), Al is chiefly present as Al^{3+} and is essentially conservative, so that the sorption of Al at pH < 5 onto hydrous iron oxides is rarely observed in nature. At higher $SO_4^=$ activities, however, the $Al(SO_4)_2^-$ species becomes important and therefore, some partial sorption of aluminum can theoretically take place at low pH if a given amount of sorbent is present in the solutions. Consequently, in the

mine waters from Lomero and Esperanza, only a minimal sorption of Al should be expected, whereas in the waters from La Zarza, Poderosa and Corta Atalaya, a more noticeable sorption of Al seems coherent.

A very similar variation of the speciation of Al(III) in relation with both pH and molality of the $SO_4^=$ ion has been already observed in acidic mine waters from the Leviathan, Hornet and Richmond mines, California, by Alpers and Nordstrom (1999) (see also Nordstrom, 2004). Using the WATEQ4F computer program (which also uses the ion-association method with an expanded form of the extended Debye-Hückel equation to calculate activity coefficients of major ions; Ball and Nordstrom, 1991), these authors obtained similar molar proportions of the $Al(SO_4)_2^-$ ion triplet (around 32% of the total dissolved Al) in waters with comparable concentrations of $SO_4^=$ and Al (for example, 50,000 and 1,410 mg/L, respectively, in their sample *AMD-C*; Alpers and Nordstrom, 1999; Nordstrom, 2004) than those found in some waters in this study (e.g., AMD from Corta Atalaya; Table I). However, as far we know, this study provides the first laboratory evidence to support that this characteristic speciation of dissolved Al can significantly affect the geochemical behavior of aluminum in acidified surface waters (by enhancing the sorption of this metal at such low pH).

With the cited exception of the water from Corta Atalaya, the obtained results have not provided any evidence for the coprecipitation of Al minerals

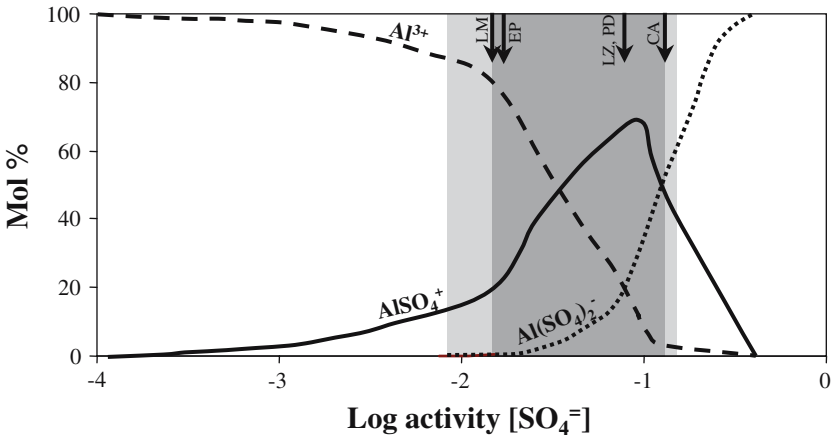

Figure 8. Variation of the aqueous speciation of Al with increasing activity of the $SO_4^=$ ion (calculations performed with the PHREEQC 2.7 code for conditions of 180 mg/L Al – median value for the IPB mine waters, taken from Sánchez-España et al., 2005a, pH = 3.5, $p\varepsilon = 13$, and $T = 25$ °C). The light-gray shaded area represents the common range of $SO_4^=$ activities for the IPB mine waters (corresponding to a concentration range of 1–45 g/L $SO_4^=$), whereas the narrower, dark-gray, shaded area indicates the range of $SO_4^=$ activities for the mine waters used in the present work (3–33 g/L $SO_4^=$). The black arrows represent the specific activities of the $SO_4^=$ ion for the studied mine waters (Lomero, LM; Esperanza, EP; La Zarza, LZ; Poderosa, PD; Corta Atalaya, CA).

along with schwertmannite. Thus, in the authors's opinion the most probable explanation for the observed Al removal is that this element has been partly sorbed by schwertmannite. This sorption of Al onto the schwertmannite colloidal particles formed at pH 2.5–3.5 (which should basically affect to the $Al(SO_4)_2^-$ complexes, as other Al ionic species such $Al(SO_4)^+$ and Al^{3+} should remain in solution) could explain the apparent drownstream decrease of the dissolved Al loadings (with a corresponding increase of the Al content in the particulate fraction) detected at nearly-constant flow rate and pH <3.5 in two acidic effluents from La Zarza and Tharsis mines (Sánchez-España et al., 2005b). It is worth to note that Chapman et al. (1983) also reported the sorption of Al by amorphous ferric hydroxide precipitating at pH 2.7–3.2 in New South Wales, Australia. Additionally, some other researchers (Yu et al., 1999; Kim and Kim, 2003; Verplanck et al., 2004) have also detected variable contents of Al_2O_3 ranging from 0.2 to 2.1%wt. in schwertmannites formed at pH 2.5–3.5, although these authors do not consider the possibility of the sorption and/or coprecipitation of Al at such low pH.

Whether the Al has been trully adsorbed onto the Fe(III) mineral sufaces or some other process has taken place (such as co-precipitation and/or cationic exchange into the schwertmannite stoichiometry) is still uncertain and requires further research. However, the results of this study suggest that the sorption of Al by schwertmannite at low pH could be, under certain conditions, more significant than it has been traditionally considered.

5. Conclusions

The oxidation and titration experiments conducted in this study show that the evolution of AMD (including oxidation of Fe(II) and neutralization with subsequent hydrolysis/precipitation of Fe(III) and Al(III) during mixing with pristine water courses) is an important hydrogeochemical process governing the transport of major and trace metals in the IPB province. Iron and aluminum are specially responsible for the scavenging of the rest of metals. The hydrolysis of Fe(III) at pH 2.5–3.5 provokes a strong buffer in the acidic solutions and leads to the formation of schwertmannite, whereas the hydrolysis of Al(III), which occurs around pH 4.5–5.0, constitutes the next buffer and leads to the precipitation of nearly amorphous Al hydroxysulphates of variable composition (commonly hydrobasaluminite or basaluminite, and more rarely aluminite).

Because of their low crystallinity, small particle size and high specific surface area, these Fe and Al mineral phases constitute ideal sorbents of trace metals dissolved in AMD. The degree of element sorption observed in the mine waters included in this study has been demonstrated to depend, among other factors, on: (i) the pH of the AMD solution (which determines the net

charge of the mineral surfaces), (ii) the amount of sorbent (precipitate) formed in the AMD solutions, (iii) the sorption affinity of the different metal ions, and (iv) the aqueous speciation of metals in the mine waters. Thus, the elements which are predominantly present in the acidic solutions as anionic species (specially As and V), can be significantly attenuated and retained in the solid phase near their sources during the oxidation of Fe(II) and the subsequent formation of schwertmannite at low pH (typically, pH <3.5). On the other hand, the metal cations (with the common sequence $Pb > Cu \approx U > Co \approx Zn > Ni \approx Mn > Cd$) are progressively sorbed by the Fe and Al phases as the solution pH is increased during neutralization of AMD by mixing with pristine waters. All these metals are mostly removed from solution in the pH range 5–7, depending on the amount of sorbent. In addition to sorption, some elements (specially Cu, but also Mn to a lesser extent) can precipitate as oxides or hydroxides at near-neutral conditions. Uranium (mainly present as U(VI)) shows an adsorption edge very similar to that of copper, and seems to be strongly sorbed by the Al and Cu compounds. Finally, at very high $SO_4^{=}$ activities (>0.1 molal), some elements like Al, Zn and Cd can form anionic bisulphate complexes which appear to have been significantly sorbed at pH <5.0.

The results show that the Al hydroxysulphates may play a more important role in the scavenging of dissolved trace metals from AMD solutions than is normally considered, although further research (which must include more detailed sorption experiments) is needed to improve the characterization of these nanocrystalline phases as sorbents of trace metals.

The combination of precipitation, sorption and dilution processes represents an important natural process of attenuation that strongly mitigates the environmental impact of the AMD pollution on rivers and water reservoirs in the province of Huelva.

Acknowledgements

This study was supported with funds from the CICYT project REN2003-09590-C O4-04, and from Junta de Andalucía (Consejería de Innovación, Ciencia y Empresa). Dr. J.A. Medina performed the SEM-EDS analyses in the Universidad Autónoma de Madrid (UAM). We appreciate the comments of an anonymous reviewer on an earlier draft of this manuscript. Finally, we thank D.K. Nordstrom for stimulating discussion on several aspects related with the geochemistry of acid mine waters.

References

Adams F. and Rawajfih Z. (1977) Basaluminite and alunite: a possible cause of sulphate retention by acid soils. *Soil. Sci. Soc. Am. J.* **41**, 686–692.

Alpers C.N. and Nordstrom D.K. (1999) Geochemical modeling of water-rock interactions in mining environments. In *The Environmental Geochemistry of Mineral Deposits, Part A. Processes, Techniques, and Health Issues* (eds. G.S. Plumlee and M.J. Logsdon), Society of Economic Geologists. *Rev. Econ. Geol.* **6A**, 289–323.

Ball, J.W. and Nordstrom D.K., 1991. User's manual for WATEQ4F with revised thermodynamic data base and test cases for calculating speciation of major, trace, and redox elements in natural waters. pp. 91–183, 189. U.S. Geological Survey Open-File Report.

Baltpurvins K. A., Burns R. C., Lawrance G. A. and Stuart A. D. (1997) Effect of Ca^{2+}, Mg^{2+}, and anion type on the aging of iron(III) hydroxide precipitates. *Environ. Sci. Technol.* **31**, 1024–1032.

Bannister F. A. and Hollingworth S. E. (1948) Basaluminite hydrobasaluminite. *Am. Mineral.* **33**, 787.

Basset H. and Goodwin T.H. (1949) The basic aluminum sulphates. *J. Chem. Soc.* 2239–2279.

Berger A. C., Bethke C. M. and Krumhans J. L. (2000) A process model of natural attenuation in drainage from a historic mining district. *Appl. Geochem.* **15**, 655–666.

Bigham J.M. and Nordstrom D.K. (2000) Iron and Aluminum Hydroxysulfates from Acid Sulfate Waters. In *Sulfate Minerals: Crystallography, Geochemistry, and Environmental Significance* (eds. C.N. Alpers, J.L. Jambor and D.K. Nordstrom). *Rev. Mineral. Geochem.* **40**, 351–403.

Bigham J. M., Schwertmann U., Traina S. J., Winland R. L. and Wolf M. (1996) Schwertmannite and the chemical modeling of iron in acid sulfate waters. *Geochim. Cosmochim. Acta* **60**, 2111–2121.

Carlson L., Bigham J. M., Schwertmann U., Kyek A. and Wagner F. (2002) Scavenging of As from acid mine drainage by schwertmannite and ferrihydrite: a comparison with synthetic analogues. *Environ. Sci. Technol.* **36**, 1712–1719.

Casiot C., Morin G., Juillot F., Bruneel O., Personné J. C., Leblanc M., Duqesne K., Bonnefoy V. and Elbaz-Poulichet (2003) Bacterial immobilization and oxidation of arsenic in acid mine drainage (Carnoulés creek, France). *Water Res.* **37**, 2929–2936 .

Chapman B. M., Jones D. R. and Jung R. F. (1983) Processes controlling metal ion attenuation in acid mine drainage streams. *Geochim. Cosmochim. Acta* **47**, 1957–1973.

Clayton T. (1980) Hydrobasaluminite and basaluminite from Chickerell, Dorset. *Mineral Mag.* **43**, 931–937.

Davis J. A. and Kent D. B. (1990). Surface complexation modeling in aqueous geochemistry, In Hochella, M. F. and White, A. F (eds.), *Mineral-Water Interface Geochemistry: Reviews in Mineralogy*. Washington, D.C.: Mineralogical Society of America, pp. 177–260 .

Dzombak D.A. and Morel F.M.M. Morel (1990) *Surface Complexation Modeling-hydrous Ferric Oxide*. John Wiley and Sons, 393 pp.

Filipek L. H., Nordstrom D. K. and Ficklin W. H. (1987) Interaction of acid mine drainage with waters and sediments of West Squaw Creek in the West Shasta Mining District, California. *Environ. Sci. Technol.* **21**, 388–396.

Fukushi K., Sasaki M., Sato T., Yanese N., Amano H. and Ikeda H. (2003) A natural attenuation of arsenic in drainage from an abandoned arsenic mine dump. *Appl. Geochem.* **18**, 1267–1278.

Fyson A. and Kalin M. (2000). Acidity titration curves – a versatile tool for the characterization of acidic mine waste water, In Friese, K. (eds.), *UFZ-Bericht*. Leipzig, Germany: Centre for Environmental Research, pp. 21–24.

Kim J. J. and Kim S. J. (2003) Environmental, mineralogical, and genetic characterization of ochreous and white precipitates from acid mine drainages in Taebaeg, Korea. *Environ. Sci Technol.* **37**, 2120–2126.

Kinniburgh D.G. and Jackson M.L. (1981) Cation adsorption by hydrous metal oxides and clay; In *Adsorption of Inorganics at Solid-Liquid Interfaces* (eds. M.A. Anderson and A.J. Rubin), pp. 91–160. Ann Arbor Science, Ann Arbor, MI.

Kinniburgh D. G., Jackson M. L. and Syers J. K. (1976) Adsorption of alkaline earth, transition, and heavy metal cations by hydrous oxide gels of iron and aluminum. *Soil Sci. Soc. Am. J.* **40**, 796–799.

Langmuir D. (1997) *Aqueous Environmental Geochemistry*. Prentice-Hall Inc., Upper Saddel River, NJ.

Leblanc M., Achard B., Ben Othman D. and Luck J. M. (1996) Accumulation of arsenic from acidic mine waters by ferruginous bacterial accretions (stromatolites). *Appl. Geochem.* **11**, 541–554.

Lee G., Bigham J. M. and Faure G. (2002) Removal of trace metals by coprecipitation with Fe, Al and Mn from natural waters contaminated with acid mine drainage in the Ducktown Mining District, Tennessee. *Appl. Geochem.* **17**, 569–581.

Nordstrom D. K. (1982) The effect of sulphate on aluminum concentrations in natural waters: some stability relations in the system Al_2O_3-SO_3-H_2O at 298 K. *Geochim. Cosmochim. Acta* **46**, 681–692.

Nordstrom D.K. (2004) Modeling low-temperature geochemical processes. In *Treatise on Geochemistry, Surface and Ground Water, Weathering, and Soils* (ex. eds. H.D. Holland and K.K. Turekian, ed. J.I. Drever), Vol. 5, pp. 37–72. Elsevier, Pergamon, Amsterdam.

Nordstrom D. K. and Ball J. W. (1986) The geochemical behavior of aluminum in acidified surface waters. *Science* **232**, 54–56.

Nordstrom D. K., Ball J. W., Robertson C. E. and Hanshaw B. B. (1984) The effect of sulphate on aluminum concentrations in natural waters: II. Field occurrences and identification of aluminum hydroxysulphate precipitates. *Geol. Soc. Am. Program Abstr.* **16**(6), 611.

Nordstrom D.K. and Alpers C.N. (1999) Geochemistry of acid mine waters. In *The Environmental Geochemistry of Mineral Deposits, Part A. Processes, Techniques, and Health Issues: Society of Economic Geologists* (eds. G.S. Plumlee and M.J. Logsdon), *Rev. Econ. Geol.* **6A**, 133–156.

Parkhurst D.L. and Appelo C.A.J. (1999) User's guide to PHREEQC (Version 2) – A computer program for speciation, batch-reaction, one-dimensional transport, and inverse geochemical calculations, pp. 99–4259. U.S. Geol. Surv. Water-Resour. Investig. Rep. Denver, Colorado.

Regenspurg S. and Peiffer S. (2005) Arsenate and chromate incorporation in schwertmannite. *Appl. Geochem.* **20**, 1226–1239.

Sánchez-España F. J., López Pamo E., Santofimia E., Aduvire O., Reyes J. and Barettino D. (2005a) Acid mine drainage in the Iberian Pyrite Belt (Odiel river watershed, Huelva, SW Spain): geochemistry, mineralogy and environmental implications. *Appl. Geochem.* **20**, 1320–1356.

Sánchez-España J., López-Pamo E., Santofimia E., Reyes J. and Martín Rubí J. A. (2005b) The natural attenuation of two acidic effluents in Tharsis and La Zarza-Perrunal mines (Iberian Pyrite Belt, Spain). *Environ. Geol.* **49**, 253–266.

Sánchez-España J., López-Pamo E., Santofimia E., Reyes J. and Martín Rubí J.A. (2006) The impact of acid mine drainage on the water quality of the Odiel river (Huelva, Spain): Evolution of Precipitate Mineralogy and Aqueous Geochemistry Along The Concepción Tintillo Segment. *Water Air Soil Pollut.* **173**, 121–149.

Sánchez España F. J., López Pamo E. and Santofimia E. (in press) The oxidation of ferrous iron in acidic mine effluents from the Iberian Pyrite Belt (Odiel Basin, Huelva, Spain): field and laboratory rates. *J. Geochem. Explor.*

Smith K.S. (1999) Metal sorption on mineral surfaces: an overview with examples relating to mineral deposits. In *The Environmental Geochemistry of Mineral Deposits, Part A. Processes, Techniques, and Health Issues: Society of Economic Geologists* (eds. G.S. Plumlee and M.J. Losdon), *Rev. Econ. Geol.* **6A**, 161–182.

Smith K.S., Ficklin W.H., Plumlee G.S. and Meier A.L. (1992) Metal and arsenic partitioning between water and suspended sediment at mine-drainage sites in diverse geologic settings; In *Water-Rock Interaction: 7th International Symposium on Water-Rock Interaction, Utah, July 13–18, 1992*, (eds. Y.K. Kharaka and A.S. Maest), pp. 443–447. Proceedings, v. 1, Rotterdam, A.A. Balkema.

Stumm W. and Morgan J. J. (1996) *Aquatic Chemistry*. 3rd ed. John Wiley & Sons Inc., New York, USA.

Totsche O., Pöthig R., Uhlmann W., Büttcher H. and Steinberg E. W. (2003) Buffering mechanisms in acidic mining lakes – A model-based analyses. *Aquat. Geochem.* **9**, 343–359.

Verplanck P. L., Nordstrom D. K., Taylor H. E. and Kimball B. A. (2004) Rare earth element partitioning between hydrous ferric oxides and acid mine water during iron oxidation. *Appl. Geochem.* **19**, 1339–1354.

Wanty R.B., Miller W.R., Briggs P.H. and McHugh J.B. (1999) Geochemical processes controlling uranium mobility in mine drainages. In *The Environmental Geochemistry of Mineral Deposits, Part A. Processes, Techniques, and Health Issues* (eds. G.S. Plumlee and M.J. Logsdon), Society of Economic Geologists, *Rev. Econ. Geol.* **6A**, 201–213.

Webster J. G., Swedlund P. J. and Webster K. S. (1998) Trace metal adsorption onto acid mine drainage Fe(III) oxyhydroxysulphate. *Environ. Sci. Technol.* **32**, 1361–1368.

Yu J., Heo B., Choi I. and Chang H. (1999) Apparent solubilities of schwertmannite and ferrihydrite in natural stream waters polluted by mine drainage. *Geochim. Cosmochim. Acta* **63**, 3407–3416.